

## Tests of QED and Elektroweak Theories at PETRA

P. Dittmann

Deutsches Elektronen-Synchrotron DESY, D-2000 Hamburg, Federal Republic of Germany

V. Hepp<sup>1</sup>

II. Institut für Experimentalphysik der Universität, D-2000 Hamburg, Federal Republic of Germany

Received 18 June 1981

**Abstract.** We review experimental results from PETRA on the reactions:  $e^+e^- \rightarrow e^+e^-$ ,  $\mu^+\mu^-$ ,  $\tau^+\tau^-$ , and  $\gamma\gamma$  at centre-of-mass energies up to 36.7 GeV. The data are compared with the predictions of quantum electrodynamics and electroweak theories. The implication of the total cross section measurements for  $e^+e^- \rightarrow q\bar{q} \rightarrow$  hadrons with respect to the weak mixing angle is discussed.

### 1. Introduction

The validity of Quantum Electrodynamics (QED) has been verified experimentally to a very high degree of accuracy. However, within the framework of unified theories which combine the effects of electromagnetic, weak and in principle also of strong interactions, corrections to QED are expected in the sense that electromagnetic reactions cannot be described by only one fixed coupling constant – the fine structure constant  $\alpha$ . In fact, the  $g-2$  experiment at CERN [1] needs the hadronic vacuum polarization caused by the strong interaction to explain its result. The SLAC asymmetry experiment [2] has measured parity violation in  $eD$  scattering which is introduced by interference of the electromagnetic and the weak interaction.

With the advent of the  $e^+e^-$  colliding beam facility PETRA at DESY tests of the validity of Quantum Electrodynamics (QED) at very large momentum transfers have become possible.  $e^+e^-$  scattering and annihilation can now be measured at centre-of-mass energies up to 36.7 GeV corresponding to momentum transfers as large as 1350 GeV<sup>2</sup> which have not been accessible up to now. For comparison, previous QED tests at SPEAR [3] and DORIS [4] covered momentum transfers up to  $\sim 50$  GeV<sup>2</sup>.

Precise tests of QED at high momentum transfers are of great importance both for atomic and for high

energy physics. High precision atomic physics experiments depend strongly on the lower bound on the cut-off parameter  $\Lambda$  when compared to unified theories. High energy experiments with colliding beams rely on the validity of QED, since all cross sections for new phenomena are normalized to Bhabha scattering. Furthermore, at the highest PETRA energies, electroweak theories like  $SU(2) \otimes U(1)$  predict measurable deviations from QED due to interference with the weak neutral current. Above all, tests of QED are of fundamental importance, because QED has been the first successful gauge theory.

This report summarizes the results obtained at PETRA on the reactions

$$\begin{aligned}
 e^+e^- &\rightarrow e^+e^- && \text{(Bhabha scattering)} \\
 e^+e^- &\rightarrow \mu^+\mu^-, \tau^+\tau^- && \text{(Lepton pair production)} \\
 e^+e^- &\rightarrow \gamma\gamma && \text{(Two photon annihilation)} \\
 e^+e^- &\rightarrow q\bar{q} \rightarrow \text{hadrons} && \text{(Total hadronic cross section).}
 \end{aligned}$$

Data were taken with the detectors JADE [5], MARK J [6], PLUTO [7], TASSO [8] and CELLO [9] at centre-of-mass energies up to 36.7 GeV. The CELLO analysis is restricted to Bhabha scattering and two photon annihilation, since this detector moved into the beam only recently. Details of the apparatus and of the experimental procedure can be found in the references. A discussion of the two-photon exchange process  $e^+e^- \rightarrow e^+e^- +$  lepton pair which occurs at predominantly low momentum transfer will be omitted from this presentation.

The report is structured as follows: Section 2 gives a review of the lowest order cross sections and the radiative corrections for the reactions mentioned above. In Sect. 3 possible modifications of QED are outlined and their effects on the cross sections are discussed. Experimental results are given in Sect. 4. The effects due to the interference of the electromagnetic and weak interactions are discussed in Sect. 5. Finally, Sect. 6 gives a summary.

<sup>1</sup> On leave of absence from University of Heidelberg

## 2. QED Cross Sections

The differential cross sections for QED reactions are usually [10] written in the form

$$\frac{d\sigma_{\text{QED}}}{d\Omega} = \frac{d\sigma_0}{d\Omega} (1 + \delta_{\text{rad}}), \quad (1)$$

where  $d\sigma_0/d\Omega$  denotes the QED cross section to lowest order in  $\alpha = e^2/4\pi = 1/137$ .  $d\sigma_{\text{QED}}/d\Omega$  incorporates the radiative corrections  $\delta_{\text{rad}}$  (the hadronic vacuum polarization is often also included in  $\delta_{\text{rad}}$ , see next section).  $d\sigma_0/d\Omega$  is given below for Bhabha scattering, lepton pair production and two photon annihilation in Lorentz invariant notation and also as function of the centre-of-mass energy  $\sqrt{s}$  and the scattering angle  $\theta$ :

$$e^+e^- \rightarrow e^+e^-: \quad \begin{array}{c} e \\ \diagdown \\ \gamma \\ \diagup \\ e \end{array} + \begin{array}{c} e \\ \diagup \\ \gamma \\ \diagdown \\ e \end{array}$$

$$\begin{aligned} \frac{d\sigma_0}{d\Omega} &= \frac{\alpha^2}{2s} \left\{ \frac{q'^4 + s^2}{q^4} + \frac{2q'^4}{q^2s} + \frac{q'^4 + q^4}{s^2} \right\} \\ &= \frac{\alpha^2}{4s} (3 + \cos^2\theta)^2 \end{aligned} \quad (2)$$

$$e^+e^- \rightarrow \mu^+\mu^-: \quad \begin{array}{c} e \\ \diagdown \\ \gamma \\ \diagup \\ e \end{array} \rightarrow \begin{array}{c} \mu \\ \diagdown \\ \gamma \\ \diagup \\ \mu \end{array}$$

$$\frac{d\sigma_0}{d\Omega} = \frac{\alpha^2}{2s} \left\{ \frac{q'^4 + q^4}{s^2} \right\} = \frac{\alpha^2}{4s} (1 + \cos^2\theta) \quad (3)$$

$$e^+e^- \rightarrow \tau^+\tau^-: \quad \begin{array}{c} e \\ \diagdown \\ \gamma \\ \diagup \\ e \end{array} \rightarrow \begin{array}{c} \tau \\ \diagdown \\ \gamma \\ \diagup \\ \tau \end{array}$$

$$\begin{aligned} \frac{d\sigma_0}{d\Omega} &= \frac{\alpha^2\beta}{2s} \left\{ \frac{q'^4 + 2(1-\beta^2)q'^2q^2 + q^4}{s^2} \right\} \\ &= \frac{\alpha^2\beta}{4s} (2 - \beta^2 \sin^2\theta) \end{aligned} \quad (4)$$

$$e^+e^- \rightarrow \gamma\gamma: \quad \begin{array}{c} e \\ \diagdown \\ \gamma \\ \diagup \\ e \end{array} + \begin{array}{c} e \\ \diagup \\ \gamma \\ \diagdown \\ e \end{array}$$

$$\frac{d\sigma_0}{d\Omega} = \frac{\alpha^2}{2s} \left\{ \frac{q'^4 + q^4}{q'^2q^2} \right\} = \frac{\alpha^2}{s} \frac{1 + \cos^2\theta}{\sin^2\theta} \quad (5)$$

with  $q^2 = -s(1 - \cos\theta)/2$ ,  $q'^2 = -s(1 + \cos\theta)/2$ ,  $\beta = p/E$ . The polar angle  $\theta$  is measured with respect to the beam axis. The initial electrons and positrons are assumed to be unpolarized. Terms of order  $m/E$  are neglected, except in (4) which includes the threshold behaviour of the lepton pair production cross section. For  $1 - \beta \ll 1$

( $m_\tau \ll E_\tau$ ) (3) and (4) become identical. The divergence of the first order Bhabha scattering cross section at  $\theta=0$  is well known. Equation (3) can be integrated over the full solid angle which leads to the total cross section for  $\mu$  pair production

$$\sigma_0(e^+e^- \rightarrow \mu^+\mu^-) = \frac{4\pi\alpha^2}{3s} \approx \frac{86.8}{s} \quad (\text{nb, } s \text{ in GeV}^2). \quad (6)$$

The amplitudes necessary to describe the reaction  $e^+e^- \rightarrow e^+e^-$  in the framework of QED up to order  $\alpha^3$  are shown as Feynman diagrams in Fig. 1. The first two diagrams stand for space- and timelike Bhabha scattering to lowest order in  $\alpha = e^2/4\pi$ . The next 8 graphs account for radiative corrections due to the emission of real photons. The following 14 graphs describe virtual radiative corrections and contribute to order  $\alpha^3$  to the cross section via interference with the two lowest order amplitudes. Of these the first 8 are vertex and two photon exchange corrections, the other 6 vacuum polarization. In  $\mu$  and  $\tau$  pair production only the timelike diagrams contribute.

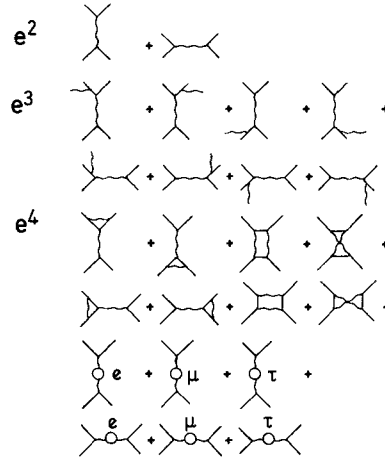


Fig. 1. QED diagrams which contribute to the cross section up to order  $\alpha^3$  for the reaction  $e^+e^- \rightarrow e^+e^-$

The radiative corrections due to initial and large angle final state radiation produce an acollinearity of the final state particles. Figure 2 shows the distribution of the acollinearity angle\* between electrons and positrons from Bhabha scattering as measured e.g. by JADE. Clearly, a cut in the acollinearity angle will lead to a loss of events. On the other hand, initial state radiation decreases the available centre-of-mass energy which leads to higher yields than expected at the nominal c.m. energies because of the  $1/s$  dependence of the cross section. The size of the radiative corrections therefore depends on the cuts in the energies and the acollinearity angle of the final state particles.

\* The acollinearity angle is usually defined as  $|\pi - \cos^{-1}(\mathbf{n}_1 \cdot \mathbf{n}_2)|$  where  $\mathbf{n}_1, \mathbf{n}_2$  are unit vectors in the direction of the two outgoing particles

The virtual radiative corrections mainly distort the angular distributions (especially the two photon exchange) and change the absolute cross sections.

The radiative corrections for Bhabha scattering, lepton pair production and two photon annihilation have been calculated up to order  $\alpha^3$  and for details we refer the reader to the literature [10–12]. Since they depend on the experimental setup we do not give precise numbers here. For  $\mu$  pair production in e.g. the PLUTO detector the radiative corrections vary between +5.4% ( $\cos\theta=0.75$ ) and -2.2% ( $\cos\theta=-0.75$ ), if the acollinearity angle is restricted to be  $<10^\circ$  and the muon momentum has to exceed 50% of the beam energy at  $\sqrt{s}=30$  GeV.

The curve in Fig. 2 is the QED prediction for Bhabha scattering including the radiative corrections and folded with the angular resolution of the detector. The excellent agreement with the data leads to the conclusion that the radiative corrections for the emission of real photons are understood, even at the highest PETRA energies.

### 3. Modification of QED

Two corrections to QED are expected to become measurable at PETRA, the hadronic vacuum polarization,  $\delta_{\text{had}}$ , and the interference of the electromagnetic and weak interaction,  $\delta_{\text{weak}}$ . Any unexpected deviation from the known theory may be incorporated into a correction  $\delta_A$ . The modified cross section then reads

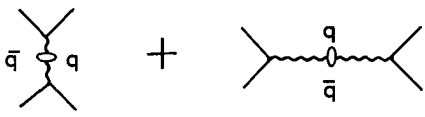
$$\frac{d\sigma}{d\Omega} = \frac{d\sigma_{\text{QED}}}{d\Omega} (1 + \delta_{\text{had}} + \delta_{\text{weak}} + \delta_A), \quad (7)$$

where  $d\sigma_{\text{QED}}/d\Omega$  is given by (1). Here and in the following it is understood that the radiative corrections to  $d\sigma/d\Omega$  had been accounted for. The modifications  $\delta$  are in general a function of the scattering angle  $\theta$  and of the centre-of-mass energy  $\sqrt{s}$ , and are assumed to be small. Their actual parameterisation will be discussed below.

#### 3.1. Hadronic Vacuum Polarization

The two graphs shown below contribute to Bhabha scattering and lepton pair production, and represent the hadronic vacuum polarization  $\Pi_h$ , which is a modification of the photon propagator.

The modification is related to the total cross section for  $e^+e^- \rightarrow \text{hadrons}$  through a dispersion relation [13]



$$\text{Re}\Pi_h(s) = \frac{s}{4\pi^2\alpha} P \int_{4m_\pi^2}^{\infty} \frac{\sigma(e^+e^- \rightarrow \text{hadrons})}{s' - s} ds', \quad (8)$$

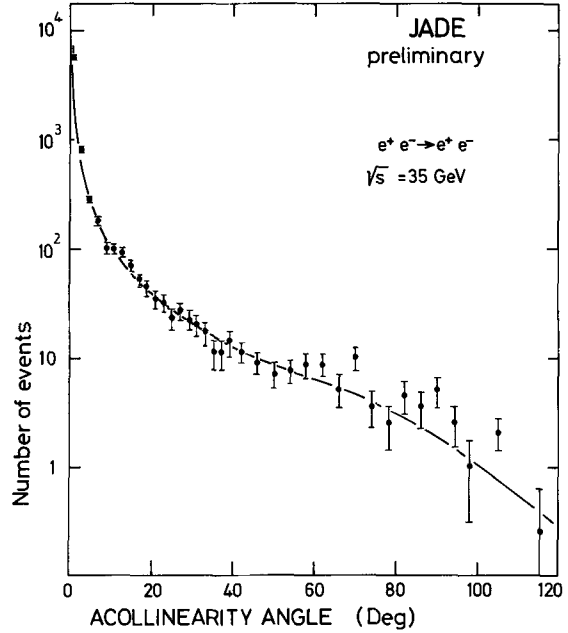


Fig. 2. Acollinearity angle distribution for Bhabha scattering. The curve shows the QED prediction folded with the angular resolution of the JADE lead glass detector

where  $s$  has to be substituted by  $q^2$  for the spacelike part. This function is tabulated in [13] using the measured total cross section with all its resonances and thresholds. Therefore it includes all presently known quarks, with their bound states, as well as higher order corrections inside the quark-loop. Numerically  $\text{Re}\Pi_h$  is mainly dominated by the hadronic cross section at low energies.

The Bhabha cross section modified for the hadronic vacuum polarization then reads (higher orders in  $\Pi_h$  neglected):

$$\frac{d\sigma}{d\Omega} = \frac{d\sigma_{\text{QED}}}{d\Omega} - \frac{\alpha^2}{s} \left\{ \frac{q'^4 + s^2}{q^4} \text{Re}\Pi_h(q^2) + \frac{q'^4}{q^2 s} (\text{Re}\Pi_h(q^2) + \text{Re}\Pi_h(s)) + \frac{q'^4 + q^4}{s^2} \text{Re}\Pi_h(s) \right\}. \quad (9)$$

After division of the second term by  $d\sigma_{\text{QED}}/d\Omega$  one obtains:

$$\delta_{\text{had}}(s, \theta) = - \frac{2}{3 + \cos^2\theta} ((3 + \cos\theta) \text{Re}\Pi_h(q^2) - \cos\theta(1 - \cos\theta) \text{Re}\Pi_h(s)). \quad (10)$$

$\delta_{\text{had}}$  is 0 at  $\theta=0^\circ$  since  $\Pi_h(0)=0$ . At  $\sqrt{s}=31$  GeV and  $\theta=180^\circ$  it reaches  $\sim 5\%$ . The functional dependence on  $\theta$  and  $\sqrt{s}$  is displayed in Fig. 3a. The values for  $\delta_{\text{had}}$  given here are smaller than those given in [13], where  $\sigma(\sqrt{s} > 5 \text{ GeV}) = 5 \cdot \sigma_{\mu\mu}$  was assumed. Using  $R=4$  as the measurements [14] at PETRA suggest,  $\delta_{\text{had}}$

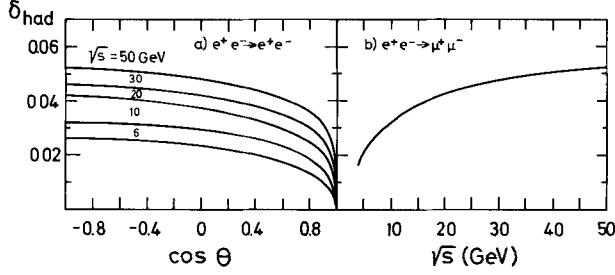


**Fig. 3 a and b.** Hadronic vacuum polarization as a function of the centre-of-mass energy for **a** Bhabha scattering and **b** muon pair production

changes by  $-0.6\%$  at  $\sqrt{s} = 31$  GeV. Further uncertainties in the calculation of  $\delta_{\text{had}}$  come from the hadronic cross section at low energies and are of the relative order of 10%, i.e.  $\delta_{\text{had}} \sim (5 \pm \sim 0.5)\%$ .

For  $\mu^+\mu^-$  and  $\tau^+\tau^-$  production one has ( $m_\tau \ll \sqrt{s}$ )

$$\frac{d\sigma}{d\Omega} = \frac{d\sigma_{\text{QED}}}{d\Omega} (1 - 2 \text{Re} \Pi_h(s)) \quad (11)$$

and

$$\delta_{\text{had}}(s) = -2 \text{Re} \Pi_h(s). \quad (12)$$

Here  $\delta_{\text{had}}$  is a function of  $s$  only and may be determined from the total cross section.  $\delta_{\text{had}}$  amounts to 4.6% at  $\sqrt{s} = 31$  GeV, see Fig. 3b.

An interesting remark can be made here. The dispersion relation (8) already knows something about the “future”, i.e. about the  $e^+e^-$  annihilation cross section at very high energies. Although this part is damped by the factor  $s' - s$  in the denominator its measurement could give some indication about the asymptotic behaviour of the total cross section. If one adds to the hadronic vacuum polarization a hypothetical part

$$\delta_{\text{had}} \rightarrow \delta_{\text{had}} + \delta'_{\text{had}}$$

one obtains, using (6) of [13]

$$\delta'_{\text{had}} = \frac{2\alpha}{3\pi} \sum_q \left( R(s_q) \ln \left| \frac{s - s_q}{s_q} \right| \right), \quad (13)$$

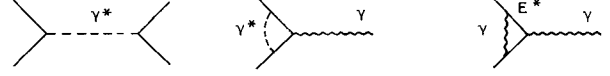
where the sum may be taken over unknown quarks.

$R = \sigma_{qq}/\sigma_{\mu\mu} \sim 3e_q^2$  is the contribution to the cross section above the threshold  $s_q$ . For  $\sqrt{s} = 31$  GeV an additional  $R = 10$  at  $\sqrt{s_q} = 40$  GeV would give  $\delta' = -1.5\%$ . Hence for quarks with usual charges such an effect is almost unmeasurable. Only huge changes in  $R$  could be detected a few GeV before the actual threshold.

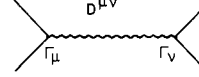
### 3.2. Cut-off Parameters in Reactions $e^+e^- \rightarrow \ell^+\ell^-$

It is customary to parameterize an unexpected deviation from the known theory of QED by cut-off parameters  $\Lambda$ . In fact,  $\Lambda$  was introduced a long time ago [15] to account for possible modifications of the

photon propagator or the lepton-photon vertices by some unknown objects. Such objects could be heavy photon-like states ( $\gamma^*$ ) or heavy electrons ( $E^*$ ) with a finite coupling strength to ordinary photons or leptons, e.g.



The matrix element  $M_{i,j}$  for Bhabha scattering is built from the vertex functions  $\Gamma_\mu = \gamma_\mu F(q^2) + (\sigma^{\mu\nu} q^\nu$  term) and the photon propagator  $D^{\mu\nu} = -D(q^2)g^{\mu\nu}/q^2$ .



The  $\sigma^{\mu\nu}q^\nu$  term is of the order of  $\sim 20\%$  in standard QED and therefore neglected in the following. The differential cross section measures the product  $|F^2 D|^2$ . The form factors  $F(q^2)$  and  $D(q^2)$  are of course unity in standard QED.

Deviations from QED can arise from a modification of the photon propagator  $D^{\mu\nu}$  for  $q^2 \neq 0$ , e.g. by a heavy photon, which may lead to the substitution

$$\begin{aligned} -\frac{1}{q^2} &\rightarrow -\frac{1}{q^2} - \frac{1}{q^2 - \Lambda_p^2} \\ &\approx -\frac{1}{q^2} \left( 1 - \frac{q^2}{\Lambda_p^2} \right) \quad \text{for } q^2/\Lambda_p^2 \ll 1. \end{aligned}$$

Similarly such a heavy photon will modify the vertex  $\Gamma_\mu$  for  $q^2 \neq 0$  for which we again keep only the first term in the expansion with respect to  $q^2$ :

$$\Gamma_\mu = \gamma_\mu F(q^2) \approx \gamma_\mu (1 + q^2/\Lambda_V^2).$$

Both modifications are usually parameterized with common form factors  $F_s, F_t$ , allowing for a difference in the spacelike (subscript  $s$ ) or timelike (subscript  $t$ ) region of four momentum transfer either by pole terms or just by the linear expansion:

$$\begin{aligned} F_s = F^2 D &= 1 \mp \frac{q^2}{q^2 - \Lambda_{\pm,s}^2} \sim 1 \pm \frac{q^2}{\Lambda_{\pm,s}^2} \\ F_t = F^2 D &= 1 \mp \frac{s}{s - \Lambda_{\pm,t}^2} \sim 1 \pm \frac{s}{\Lambda_{\pm,t}^2}. \end{aligned} \quad (14)$$

Note that  $\Lambda_\pm$  describes globally the effect due to  $\Lambda_V$  or  $\Lambda_p$ , and that these form factors are valid approximations only for small deviations from unity [16]. For  $\Lambda_t$  the subscript  $\pm$  refers to the sign of the correction, but not for  $\Lambda_s$  due to  $q^2 < 0$ .

The introduction of the form factors (14) into the lowest order amplitudes then modifies the differential Bhabha scattering cross section:

$$\begin{aligned} \frac{d\sigma}{d\Omega} &= \frac{\alpha^2}{2s} \left\{ \frac{q'^4 + s^2}{q^4} |F_s(q^2)|^2 \right. \\ &\quad \left. + \frac{2q'^4}{q^2 s} \text{Re}(F_s(q^2)F_t^*(s)) + \frac{q'^4 + q^4}{s^2} |F_t(s)|^2 \right\}. \end{aligned} \quad (15)$$

After some algebra, setting  $A_s = A_t$  and neglecting higher orders in  $1/\Lambda^2$  one obtains

$$\delta_A(s, \theta) = \mp \frac{3s}{A_{\pm}^2} \frac{1 - \cos^2 \theta}{3 + \cos^2 \theta}. \quad (16)$$

This expression can be put into the cross section (7) and compared to measured data.  $\delta_A$  is zero at  $\theta = 0^\circ$  and roughly symmetric around  $\theta = 90^\circ$ . For  $\Lambda = 100$  GeV and  $\sqrt{s} = 31$  GeV  $\delta_A$  amounts to 10% at  $\theta = 90^\circ$ , see Fig. 4a.

In the case of  $\mu$  and  $\tau$  pair production where only timelike amplitudes contribute the differential cross section reads ( $m_t \ll \sqrt{s}$ )

$$\frac{d\sigma}{d\Omega} = \frac{\alpha^2}{4s} (1 + \cos^2 \theta) |F_t(s)|^2 \quad (17)$$

and

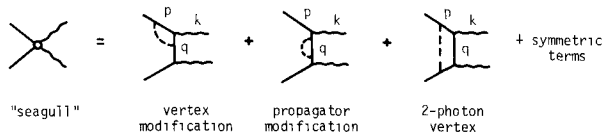
$$\delta_A(s) = \pm \frac{2s}{A_{\pm}^2}. \quad (18)$$

Here  $\delta_A$  is independent of  $\theta$ . For  $\Lambda = 100$  GeV,  $\sqrt{s} = 31$  GeV,  $\delta_A$  is 20% (Fig. 4b). Note that in case of Bhabha scattering lower limits on  $\Lambda$  are deduced from the angular distribution, but in the case of pair production they are obtained from the integrated cross section.

### 3.3. Cut-off Parameter in the Reaction $e^+e^- \rightarrow \gamma\gamma$

In two photon annihilation the hadronic vacuum polarization and electroweak interference have no effect. Tests however can be made for the existence of heavy objects,  $E^*$ , which couple to the electron or photon. Two approaches are known: contributions from the "seagull" graph [16] and heavy electron exchange [17]. Both QED modifications show up only in  $O(q^4/\Lambda^4)$ .

We will first discuss the "seagull" graph and illustrate the cancellation of the  $O(q^2/\Lambda^2)$  terms by looking at a simple set of diagrams



The dashed lines symbolize the coupling of a new neutral object to the fermions. In this case gauge invariance gives an important constraint to the  $q^2$  dependence of the modification. The Ward-Takahashi-identity [18] relates the divergence of the vertex function to the fermion propagators  $S_F$ :

$$k^\mu \Gamma_\mu(q) = S_F^{-1}(p) - S_F^{-1}(q)$$

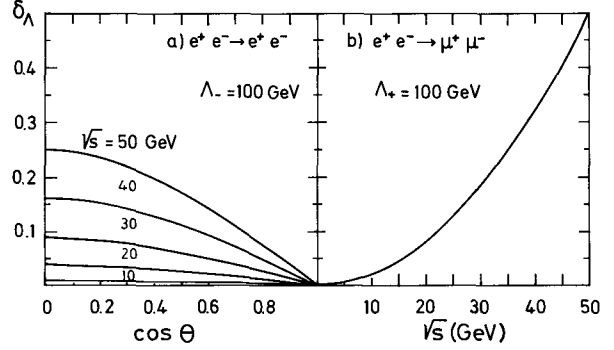


Fig. 4 a and b. The correction term  $\delta_A$  for  $\Lambda = 100$  GeV as a function of the centre-of-mass energy for a Bhabha scattering and b muon pair production

with  $S_F(p) = 1/(p - m)$ .  $p, q, k$  are the four momenta of the real and virtual lepton and real photon, respectively. Since the momentum  $p$  is on-shell ( $p = m; S_F^{-1}(p) = 0$ ) it may be written as:

$$k^\mu \Gamma_\mu(q) S_F(q) = -1.$$

If we approximate  $\Gamma_\mu(q) = \gamma_\mu F(q^2)$  we obtain:

$$k^\mu \gamma_\mu F(q^2) S_F(q) = -1 \quad \text{or} \quad F(q^2) S_F(q) = \frac{1}{\not{q} - m},$$

i.e. the modification cancels completely for one vertex and the adjacent propagator.

The Ward-Takahashi-identity gives no restriction on the  $\sigma_\mu, k^\nu$  term of the vertex which effectively contributes also only in  $O(q^4/\Lambda^4)$ .

For the second vertex there are still cancellations against the "two photon vertex" (see above diagrams). It can be shown [16, 19] that all corrections  $O(q^2/\Lambda^2)$  cancel and that the modification can be parameterized by form factors:

$$F(q^2) \approx 1 \pm \frac{q^4}{\Lambda_{\pm}^4}.$$

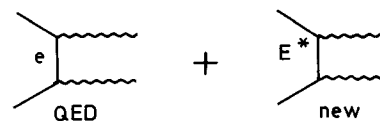
Hence:

$$\frac{d\sigma}{d\Omega} = \frac{\alpha^2}{2s} \left\{ \frac{q'^2}{q^2} |F(q^2)|^2 + \frac{q^2}{q'^2} |F(q')|^2 \right\} \quad (19)$$

and with  $F(q^2)$  as given above

$$\delta_A(s, \theta) = \pm \frac{s^2}{2\Lambda_{\pm}^4} \frac{\sin^4 \theta}{1 + \cos^2 \theta}. \quad (20)$$

In the case of heavy electron exchange we consider the interference of two amplitudes:



Current conservation excludes a  $\gamma_\mu$  coupling between  $e$ ,  $E^*$ , and  $\gamma$ . The allowed magnetic moment coupling leads for dimensional reasons to a matrix element  $M_{if}(E^*)$  of the approximate form

$$M_{if}(E^*) \approx \frac{e^{*2}}{m_{E^*}^2} \frac{s}{q^2 - m_{E^*}^2},$$

$m_{E^*}$  = mass of heavy electron

where we have written the magnetic transition moment as  $e^*/m_{E^*}$ . The QED matrix element  $M_{if}(e)$  is proportional to  $e^2/(q^2 - m_e^2)$ . Hence we expect qualitatively for  $m_e^2 \ll q^2 \ll m_{E^*}^2$ :

$$\begin{aligned} \frac{M_{if}(E^*)}{M_{if}(e)} &\sim \frac{\delta_A}{2} \sim \frac{e^{*2}}{e^2 m_{E^*}^2} \frac{q^2}{-m_{E^*}^2} s \\ &\sim \frac{e^{*2}}{e^2 m_{E^*}^4} s^2 \sin^2 \theta / 2. \end{aligned}$$

A quantitative calculation of the cross section [17] yields:

$$\frac{d\sigma}{d\Omega} = \frac{\alpha^2}{s} \frac{1 + \cos^2 \theta}{\sin^2 \theta} \left( 1 + \frac{s^2}{2\Lambda^4} \sin^2 \theta \right) \quad (21)$$

Here  $\Lambda = m_{E^*} \sqrt{e/e^*}$  signifies the mass of the heavy electron  $E^*$  if the coupling  $e^*$  is equal to  $e$ . Division by the lowest order cross section leads to

$$\delta_A(s, \theta) = \frac{s^2}{2\Lambda^4} \sin^2 \theta = \frac{s^2}{2\Lambda^4} \frac{\sin^4 \theta}{1 - \cos^2 \theta}. \quad (22)$$

In both cases, (20) and (22), the modifications at  $\theta = 90^\circ$  are of equal size and maximum. They are numerically smaller than in the case of Bhabha scattering or lepton pair production. At  $\sqrt{s} = 31$  GeV and  $\theta = 90^\circ$  a value of  $\Lambda = 40$  GeV gives  $\delta = 20\%$  ( $\sqrt{s}/\Lambda = 0.6$ ). In Fig. 5 values for  $\delta_A$  are displayed for  $\sqrt{s}/\Lambda = 1$ .

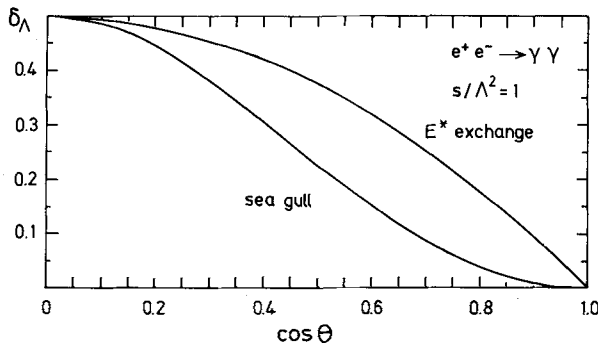


Fig. 5. The correction term  $\delta_A$  in two photon annihilation for  $s/\Lambda^2 = 1$

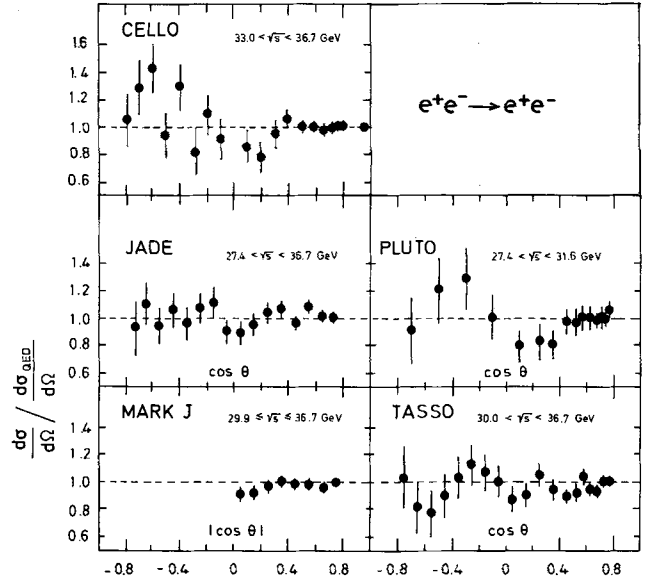


Fig. 6. Differential cross section for the reaction  $e^+e^- \rightarrow e^+e^-$  divided by the QED prediction. The data are corrected for radiative effects and hadronic vacuum polarization

#### 4. Experimental Results

Bhabha scattering,  $\mu\mu$  and  $\tau\tau$  pair production and two photon annihilation have been studied by four experiments at PETRA, i.e. the JADE [20], MARK J [21], PLUTO [22] and TASSO [23] collaborations. The CELLO group [24] has reported results on Bhabha scattering and two photon annihilation. The differential cross sections are available from  $\sqrt{s} = 12$  GeV up to  $\sqrt{s} = 36.7$  GeV. Since PETRA is continuously producing more luminosity at increasingly higher energies, the results shown below are a snapshot of the current evaluation of the data. For completeness, we have included the PLUTO data at  $\sqrt{s} = 9.46$  GeV which were actually taken at DORIS.

To display the data we have divided the measured cross sections by the 1st order QED prediction. The experimental cross sections have already been corrected for radiative effects and hadronic vacuum polarization. This procedure allows a comparison of different experiments and also a direct comparison with the deviations  $\delta$  as discussed in the previous section. On the other hand, we did not try to combine the data of different experiments since systematic errors in the data are not negligible and could easily have the same origin.

##### 4.1. $e^+e^- \rightarrow e^+e^-$

In Fig. 6 the differential cross sections are given for a wide range of energies. The data from the MARK J

experiment are not charge separated, whereas those from CELLO, JADE, PLUTO and TASSO are. The agreement with QED is very impressive at all energies and scattering angles.

The experiments have fitted  $\delta_A$ , (16), and derived lower bounds on  $\Lambda$  which are summarized in Table 1. These bounds are defined as lower limits for  $\Lambda$  at the 95% confidence level. Qualitatively, the limits on  $\Lambda$  are obtained by varying  $\delta = (\sigma - \sigma_{\text{QED}})/\sigma_{\text{QED}}$  within 2 standard deviations. In all five experiments the precision in the determination of  $\delta$  is limited by systematic errors of  $\sim 3\%$  due to the fact that the data are normalized to QED at small angles. Then with the help of (16),  $\delta \sim 0.06 \sim s/\Lambda^2$  leads to  $\Lambda \sim 140$  GeV. (More rigorous methods of obtaining the 95% confidence level lead to slightly smaller values for  $\Lambda$ .) Sometimes asymmetric values for  $\Lambda_+$  and  $\Lambda_-$  are obtained. This happens if an experiment measures a difference between theory and experiment, say  $(4 \pm 4)\%$ . Then, with the same reasoning as above, one would obtain  $\Lambda_+ = 170$  GeV and  $\Lambda_- = 100$  GeV.

The PLUTO and TASSO collaborations have used their measurements in the full accessible angular range to determine  $\Lambda_s$  and  $\Lambda_t$  separately. The results show no deviation from crossing symmetry.

We have mentioned above already the effect of systematic errors on the determination of  $\Lambda$ . Such uncertainties, however, are hard to exclude due to the usual problems with normalization (luminosity), background and experimental acceptance and are in the order of 2–4%. Another reason for a systematic effect in the determination of  $\Lambda$  and its bounds would be a longitudinal beam polarization  $P_{\parallel}$ . Although one expects only transverse polarized beams in an ideal  $e^+e^-$  storage ring, field irregularities might produce spin vectors with small longitudinal components. A longitudinal polarization would decrease the QED cross sections for lepton pair production and annihilation into photons, (3)–(6), by a factor  $(1 - P_{\parallel}^2)$ . In the case of Bhabha scattering the cross section would increase as a function of  $\theta$  [25]. In analogy to Sect. 3 we have calculated  $\delta_{\text{pol}}$  for Bhabha scattering (averaged over the azimuthal angle and hence removed the transverse polarization part)

$$\delta_{\text{pol}}(\theta) = P_{\parallel}^2 \left( \frac{16}{(3 + \cos^2 \theta)^2} - 1 \right). \quad (23)$$

$\delta_{\text{pol}}$  is symmetric around  $\theta = 90^\circ$  and vanishes at  $\theta = 0^\circ$  and  $180^\circ$ . Figure 7 shows this behaviour in graphical form for some values of  $P_{\parallel}$ .

The  $\theta$ -dependence of  $\delta_{\text{pol}}$  and  $\delta_A$ , (16), is very similar and allows a direct comparison. Thus, if  $\Lambda > 120$  GeV at  $\sqrt{s} = 35$  GeV, then  $P_{\parallel} \lesssim 0.3$  with 95% C.L. It should be mentioned that the experiments

**Table 1.** QED cut-off parameters in GeV (95% C.L.) from Bhabha scattering at  $\sqrt{s} \sim 35$  GeV (PLUTO,  $\sqrt{s} < 31.6$  GeV) For the definition of  $\Lambda_{\pm}$  see references

Group	$\Lambda_+$	$\Lambda_-$	Ref
CELLO	> 83	> 155	[24]
JADE	> 112	> 106	[20]
MARK J	> 96	> 179	[21]
PLUTO	> 80	> 234	[22]
TASSO	> 150	> 136	[23]

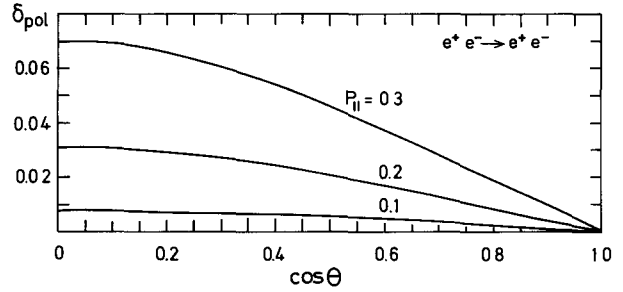


**Fig. 7.** The effect of a longitudinal beam polarization on Bhabha scattering

have, of course, inspected the azimuthal distributions where effects from transverse polarization should show up. No indication of transverse polarization has been found.

Finally, in the discussion of systematic effects, we note that the cut-off parameters as given in Table 1 were determined ignoring  $\delta_{\text{weak}}$  in (7). The electroweak effect is calculable in the framework of the Weinberg-Salam model and is about  $-3\%$  at  $\sqrt{s} = 35$  GeV (see next section).

Inspecting Table 1 we can estimate  $\Lambda$  conservatively to be  $> 120$  GeV. We do not convert this limit into a limit on the charge radius of the electron since the relation is not straightforward [10]. But for people who prefer a geometrical interpretation, one may conclude that QED has been tested successfully to distances  $r \sim 1/\sqrt{|q_{\text{max}}^2|} \sim 6 \cdot 10^{-16}$  cm.

#### 4.2. $e^+e^- \rightarrow \mu^+\mu^-$

Since  $\mu^+\mu^-$  production proceeds only through the timelike photon exchange, the cross section is much smaller than for Bhabha scattering. Figure 8 shows the total experimental cross section divided by the QED prediction as a function of the centre-of-mass energy. From these ratios the experiments have derived lower limits on  $\Lambda$ , using (18). These are given in Table 2. Despite the much poorer statistics they are similar to those obtained from Bhabha scattering because the

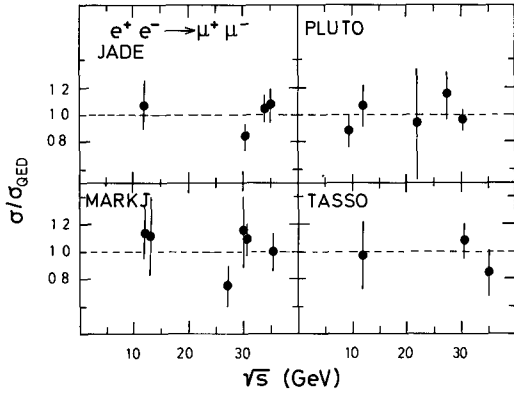


Fig. 8. Total cross section for the reaction  $e^+e^- \rightarrow \mu^+\mu^-$  divided by the QED prediction. The data are corrected for radiative effects and hadronic vacuum polarization

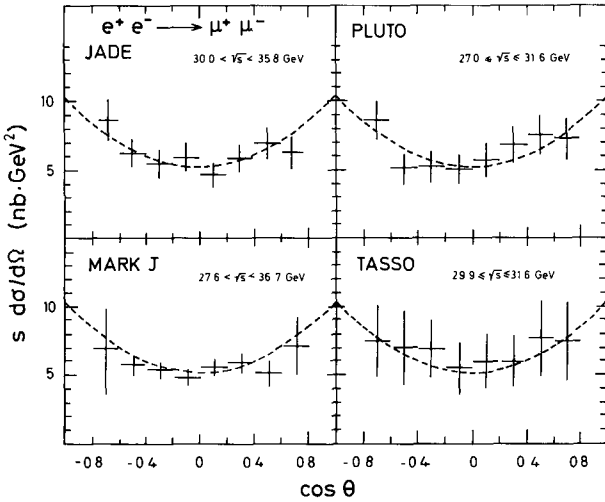


Fig. 9. Differential cross section for the reaction  $e^+e^- \rightarrow \mu^+\mu^-$ . The dashed curves show the QED prediction. The data are corrected for radiative effects and hadronic vacuum polarization

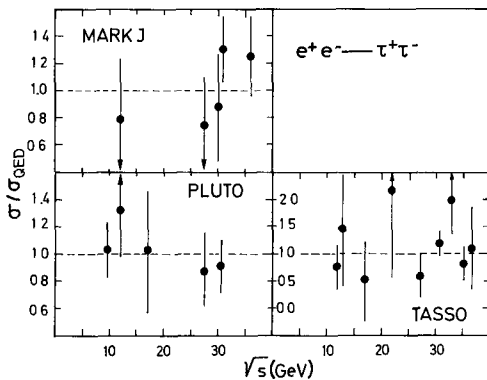


Fig. 10. Total cross section for the reaction  $e^+e^- \rightarrow \tau^+\tau^-$  divided by the QED prediction. The data are corrected for radiative effects and hadronic vacuum polarization

Table 2. QED cut-off parameters in GeV (95% C.L.) from  $\mu^+\mu^-$  pair production at  $\sqrt{s} \sim 35$  GeV (PLUTO  $\sqrt{s} < 31.6$  GeV) For the definition of  $A_{\pm}$  see references

Group	$A_+$	$A_-$	Ref.
JADE	$> 142$	$> 126$	[20]
MARK J	$> 194$	$> 153$	[21]
PLUTO	$> 107$	$> 101$	[22]
TASSO	$> 80$	$> 118$	[23]

Table 3. Angular asymmetry of  $\mu^+\mu^-$  pair production at  $\sqrt{s} = 35$  GeV (PLUTO  $\sqrt{s} < 31.6$  GeV)

Group	$A$	Ref.
JADE	$-0.05 \pm 0.06$	[20]
MARK J	$-0.01 \pm 0.06$	[21]
PLUTO	$0.07 \pm 0.10$	[22]
TASSO	$-0.06 \pm 0.08$	[23]

timelike annihilation provides maximum  $q^2$  over the full angular range. A good average of the lower limits is again  $A > 120$  GeV.

As mentioned in Sect. 3.1 the hadronic vacuum polarization contains a part which is determined by the hadronic annihilation cross section at energies larger than  $\sqrt{s}$ . In the determination of the  $A$ 's, the hadronic vacuum polarization, as given by (12), was taken into account. From  $A > 120$  GeV it follows that  $\delta < 17\%$ , with 95% confidence, and therefore  $\delta'_{\text{had}} < 17\%$  in (13). However, this limit is not particularly stringent, and the situation is not likely to change in the foreseeable future.

Figure 9 shows the angular distribution  $d\sigma_0/d\Omega$  for the highest energies as measured by the four experiments. The dashed curves show the QED prediction.

The  $\mu^+\mu^-$  angular distribution is of special importance when testing electroweak effects in QED (see next section). Electroweak theories predict at  $\sqrt{s} = 35$  GeV an angular asymmetry of about  $-6\%$  within the covered  $\theta$  range. The asymmetry  $A$  is defined as:  $A = (F - B)/(F + B)$ , where  $F$  denotes the differential cross section integrated over  $\theta_1 < \theta < \theta_2$  and  $B$  the one integrated over  $\pi - \theta_2 < \theta < \pi - \theta_1$ . The values are listed in Table 3 and show that more data are desirable.

### 4.3. $e^+e^- \rightarrow \tau^+\tau^-$

Since only selected  $\tau$ -decay topologies are usually analyzed, additional uncertainties in the cross section determination arise due to assumptions on branching fractions. The total cross section for  $\tau$  pair production has been measured by the MARK J, PLUTO and TASSO experiments and is shown in Fig. 10 as a



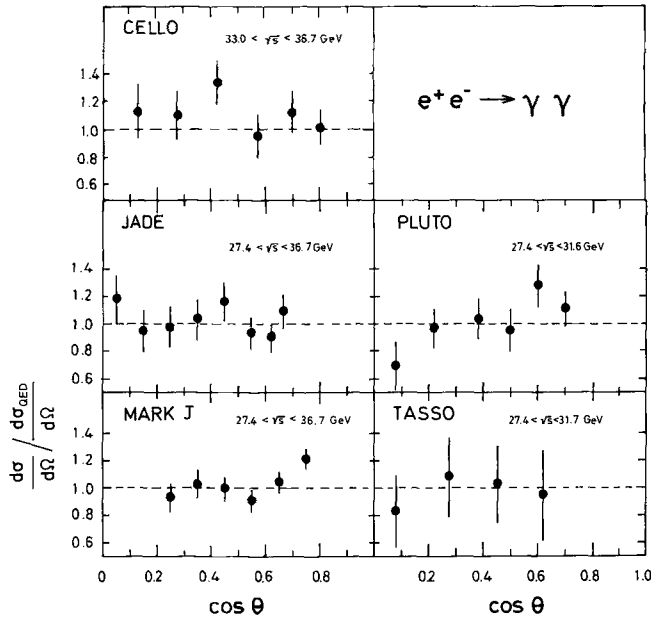


Fig. 11. Differential cross section for the reaction  $e^+e^- \rightarrow \gamma\gamma$  divided by the QED prediction. The data are corrected for radiative effects

function of  $\sqrt{s}$ . The data nicely follow the predicted cross section for a spin 1/2 pointlike lepton. In the same way as in  $\mu$  pair production the cut-off parameters  $A$  can be determined. They are given in Table 4. TASSO [23] and PLUTO [22], in addition, have measured decay branching ratios and found agreement with those measured at lower energies. By inspection of the vertex distribution of the  $\tau$  events the TASSO group was also able to give an upper limit on the  $\tau$  lifetime, of  $\tau < 1.4 \cdot 10^{-12}$  s with 95% confidence. This value is about a factor of 2 better than the previous limit from DELCO [26], but still a factor 5 from the expected lifetime of  $3 \cdot 10^{-13}$  s.

#### 4.4. $e^+e^- \rightarrow \gamma\gamma$

$e^+e^-$  annihilation into two photons has been measured by all five experiments. The differential cross section is shown in Fig. 11 and is compared to the QED prediction. The  $A$ 's are calculated using the parameterisation of (20) and (22). They are given in Table 5. Notice that, due to the parameterisation  $\delta \sim s^2/A^4$ , a much smaller value of  $A$  produces here the same effect as e.g.  $A=120$  GeV in the case of  $\mu$  pair production. The results show no deviation from QED and the mass of a heavy electron  $E^*$ , if it exists with natural coupling strength to the  $e, \gamma$ -system, must be greater than 45 GeV. Since the two photon annihilation is not subject to the electroweak interference in

Table 4. QED cut-off parameters in GeV (95% C.L.) from  $\tau^+\tau^-$  pair production at  $\sqrt{s} \sim 35$  GeV (PLUTO  $\sqrt{s} < 31.6$  GeV). For the definition of  $A_{\pm}$  see references

Group	$A_+$	$A_-$	Ref.
MARK J	> 126	> 116	[21]
PLUTO	> 79	> 63	[22]
TASSO	> 88	> 103	[23]

Table 5. QED cut-off parameters in GeV (95% C.L.) from annihilation into  $\gamma\gamma$  at  $\sqrt{s} \sim 35$  GeV (PLUTO  $\sqrt{s} < 31.6$  GeV). For the definition of  $A_{\pm}$  see references

Group	"Seagull"		Heavy electron		Ref.
	$A_+$	$A_-$	$A_+$	$A_-$	
CELLO			> 43	> 48	[24]
JADE			> 47	> 44	[20]
MARK J	> 51	> 41	> 51	> 49	[21]
PLUTO	> 46	> 36	> 46	> 42	[22]
TASSO			> 34	> 42	[23]

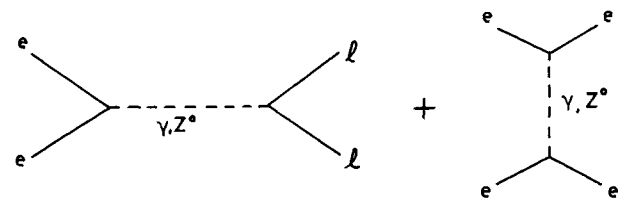
first and second order QED, it may serve as a QED test reaction at yet higher energies than at PETRA (e.g. at LEP).

## 5. Electroweak Effects

As already mentioned in Sect. 3 the weak interaction is expected to modify the QED predictions at the highest accessible PETRA energies. These corrections to QED are of the order of several percent at  $\sqrt{s} = 35$  GeV and have to be accounted for in the data analysis. Moreover, since the weak contributions to the cross sections are proportional to  $s$ , whereas the QED cross sections have a  $1/s$  energy dependence, the weak interaction will eventually dominate  $e^+e^-$  annihilation processes at sufficiently high energies [27].

### 5.1. Theories with one Neutral Vector Boson

In the unified gauge theory  $SU(2) \otimes U(1)$  the combined effect of electromagnetic and weak interactions is described via photon and neutral vector boson,  $Z^0$ , exchange according to the diagrams:



The scattering amplitude  $M$  consists of a timelike part  $M_t$  and a spacelike part  $M_s$  and, assuming  $\mu$ - $e$  universality, can be written as [28]

$$\begin{aligned}
M &= M_t + M_s \\
M_t &= -\frac{4\pi\alpha}{s} \bar{\ell} \gamma_\mu \ell \bar{e} \gamma^\mu e \\
&\quad - \frac{1}{s-m_z^2} \bar{\ell} \gamma_\mu (G_V + G_A \gamma_5) \ell \bar{e} \gamma^\mu (G_V + G_A \gamma_5) e \quad (24) \\
M_s &= \frac{4\pi\alpha}{q^2} \bar{\ell} \gamma_\mu e \bar{e} \gamma^\mu \ell \\
&\quad + \frac{1}{q^2 - m_z^2} \bar{\ell} \gamma_\mu (G_V + G_A \gamma_5) e \bar{e} \gamma^\mu (G_V + G_A \gamma_5) \ell.
\end{aligned}$$

$e$  and  $\ell$  denote the appropriate spinors of the initial and final state leptons and  $\ell = e, \mu, \tau$  with  $M_s = 0$  for  $\ell = \mu, \tau$ .  $G_V$  and  $G_A$  are the dimensionless vector and axial vector coupling constants,  $m_z$  the mass of the  $Z^0$  boson.

For historical reasons one usually identifies  $G_V$  and  $G_A$  to be in accordance with the familiar low energy 4-fermion interaction ( $s, |q^2| \ll m_z$ )

$$\begin{aligned}
\frac{G_V^2}{m_z^2} &= \frac{2G_F}{\sqrt{2}} g_V^2 = \frac{G_F}{2\sqrt{2}} v^2, \\
\frac{G_A^2}{m_z^2} &= \frac{2G_F}{\sqrt{2}} g_A^2 = \frac{G_F}{2\sqrt{2}} a^2. \quad (24a)
\end{aligned}$$

$G_F = 1.02 \times 10^{-5} m_p^{-2}$  is the Fermi coupling constant,  $g_V$  and  $g_A$  are the vector and axial vector coupling constants frequently used in neutrino scattering experiments. For the sake of simplicity the formulae given below are expressed in terms of  $v$  and  $a$ .

The scattering amplitude (24) leads to the following differential cross section for Bhabha scattering (terms of the order  $m_e/E$  neglected) [28]

$$\begin{aligned}
\frac{d\sigma}{d\Omega} &= \frac{\alpha^2}{2s} \left\{ \frac{q'^4 + s^2}{q^4} (1 + 2v^2 Q + (v^2 + a^2)^2 Q^2) \right. \\
&\quad + \frac{2q'^4}{sq^2} (1 + (v^2 + a^2)(R + Q) + (v^4 + 6v^2 a^2 + a^4) R Q) \\
&\quad + \frac{q'^4 + q^4}{s^2} (1 + 2v^2 R + (v^2 + a^2)^2 R^2) \\
&\quad + 2a^2 Q (1 + 2v^2 Q) \left( 1 + \frac{2s}{q^2} \right) \\
&\quad \left. + 2a^2 R (1 + 2v^2 R) \left( 1 + \frac{2q^2}{s} \right) \right\} \quad (25)
\end{aligned}$$

$$\begin{aligned}
&= \frac{\alpha^2}{4s} \left\{ \left( \frac{3+x^2}{1-x} \right)^2 \right. \\
&\quad + 2 \frac{3+x^2}{(1-x)^2} \{ (3+x)Q - x(1-x)R \} v^2 \\
&\quad - \frac{2}{1-x} \{ (7+4x+x^2)Q + (1+3x^2)R \} a^2 \\
&\quad + \frac{1}{2} \left\{ \frac{16}{(1-x)^2} Q^2 + (1-x)^2 R^2 \right\} (v^2 - a^2)^2 \\
&\quad \left. + \frac{1}{2} (1+x)^2 \left\{ \left( \frac{2}{1-x} Q - R \right) \right\}^2 (v^4 + 6v^2 a^2 + a^4) \right\}
\end{aligned}$$

with  $q^2 = -s(1-x)/2$ ,  $q'^2 = -s(1+x)/2$  and  $x = \cos\theta$ .

For  $\mu$  and  $\tau$  pair production the differential cross section becomes [28] ( $m_\tau \ll \sqrt{s}$ )

$$\begin{aligned}
\frac{d\sigma}{d\Omega} &= \frac{\alpha^2}{4s} \{ (1 + \cos^2\theta) (1 + 2v^2 R + (v^2 + a^2)^2 R^2) \\
&\quad + 4 \cos\theta (a^2 R + 2v^2 a^2 R^2) \} \quad (26)
\end{aligned}$$

and the total cross section

$$\sigma = \frac{4\pi\alpha^2}{3s} \{ 1 + 2v^2 R + (v^2 + a^2)^2 R^2 \}. \quad (27)$$

In the cross sections given above the square of the photon propagator was factored out of  $Q$  and  $R$ . Neglecting\* the width  $\Gamma_z$  of the  $Z^0$ ,  $Q$  and  $R$  are given by

$$Q = gm_z^2 \frac{q^2}{q^2 - m_z^2}, \quad R = gm_z^2 \frac{s}{s - m_z^2} \quad (28)$$

and

$$g = \frac{G_F}{8\sqrt{2}\pi\alpha} = 4.49 \cdot 10^{-5} \text{ GeV}^{-2}.$$

For  $s, |q^2| \ll m_z^2$  we have  $Q \sim -gq^2$ ,  $R \sim -gs$ . At PETRA energies this approximation changes  $R$  already by  $\sim 20\%$  and should not be used.

In (25)–(27), the terms independent of  $Q$  and  $R$  correspond to the pure QED contributions, the terms linear in  $Q$  and  $R$  result from electroweak interference and the terms in  $Q^2$  and  $R^2$  describe the direct contribution of the weak neutral current. The contribution of the pure weak term is proportional to  $s$  for  $s, |q^2| \ll m_z^2$  as expected for a pointlike coupling.

The differential cross sections for Bhabha scattering and lepton pair production depend on  $m_z$ ,  $g_V^2$ ,  $g_A^2$ , but not on the sign of the coupling constants since they are integrated over parity violating polarization terms. The interference term in (26) produces an angular asymmetry in lepton pair production. To measure

\* For quantitative computations near the  $Z^0$ -pole the width  $\Gamma_z$  cannot be neglected and  $R$  and  $R^2$  have to be multiplied by  $(s - m_z^2)^2 / [(s - m_z^2)^2 + \Gamma_z^2 m_z^2]$

angular asymmetries in low statistics experiments one usually calculates the integrated forward-backward asymmetry

$$A = \frac{F-B}{F+B} = \frac{6x_1^2}{3x_1+x_1^3} \frac{a^2 R + 2v^2 a^2 R^2}{1+2v^2 R + (v^2+a^2)R^2}, \quad (29)$$

where  $-x_1 < \cos\theta < x_1$  corresponds to the polar acceptance interval. For  $x_1=1$  and  $v^2 \ll a^2$ :  $A \sim 3a^2 R/2$ , and at  $\sqrt{s}=35$  GeV and  $a^2=1$ :  $A \sim -10\%$ .

In order to express more clearly the deviations from QED which are introduced by the weak interaction we take a similar approach as in Sect. 3. We use (7) with  $\delta_A=0$  and the hadronic vacuum polarization incorporated in  $\sigma_{\text{QED}}$ . We then obtain for  $e^+e^- \rightarrow e^+e^-$  ( $x = \cos\theta$ ):

$$\begin{aligned} \delta_{\text{weak}}(s, \theta) = & \frac{2}{3+x^2} \{(3+x)Q - x(1-x)R\}v^2 \\ & - \frac{2(1-x)}{(3+x^2)^2} \{(7+4x+x^2)Q + (1+3x^2)R\}a^2 \\ & + \frac{2}{(3+x^2)^2} \{(4+(1+x)^2)Q^2 \\ & + \frac{1}{2}(1-x)^2(1+x^2)R^2 \\ & - (1-x^2)(1+x)QR\}(v^2+a^2)^2 \\ & + \frac{2}{(3+x^2)^2} \{(x-1)(3+x)Q^2 + x(1-x)^2R^2 \\ & - (1-x^2)(1+x)QR\}4v^2a^2 \end{aligned} \quad (30)$$

and for  $e^+e^- \rightarrow \mu^+\mu^-, \tau^+\tau^-$

$$\begin{aligned} \delta_{\text{weak}}(s, \theta) = & R \left( 2v^2 + \frac{4 \cos\theta}{1 + \cos^2\theta} a^2 \right) \\ & + R^2 \left( (v^2 + a^2)^2 + \frac{4 \cos\theta}{1 + \cos^2\theta} 2v^2 a^2 \right). \end{aligned} \quad (31)$$

Note that there is no combination of  $v^2$  and  $a^2$  directly related to  $\delta_A$  (see Sect. 3). We want to demonstrate this explicitly for the total  $\mu$  pair cross section. Equation (31) integrated over  $\theta$  leads to ( $s \ll m_z^2$ )

$$\delta_{\text{weak}}(s) = -2gsv^2 + g^2s^2(v^2 + a^2)^2. \quad (32)$$

A comparison with (18)

$$\delta_{A_-}(s) = -2s/A_-^2 = -2s/A_-^2 + s^2/A_-^4$$

shows that because of the  $s^2$ -dependence in (32) both equations cannot be fulfilled simultaneously, except if  $a^2=0$ . Especially if  $a^2=1$  and  $v^2 < a^2$  (see below) the  $a^4 R^2$  terms in (30)–(32) are of the same order of magnitude as the  $v^2 R$  terms at  $\sqrt{s}=35$  GeV and cannot be neglected. The  $s^2/A_-^4$  term in (18) can always be neglected, and actually was neglected in Sect. 3. Thus, a limit on  $\delta_A$  implies a limit on  $\delta_{\text{weak}}$ , but this limit cannot easily be converted into a limit on  $v^2$ .

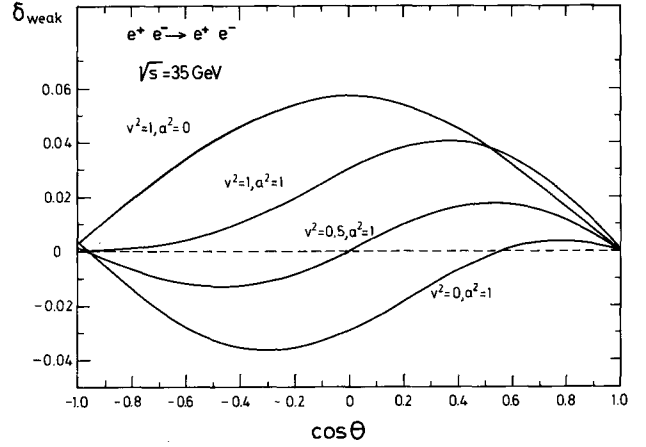


Fig. 12. The correction term  $\delta_{\text{weak}}$  in Bhabha scattering for various values of  $v^2=4g_V^2$  and  $a^2=4g_A^2$  at  $\sqrt{s}=35$  GeV

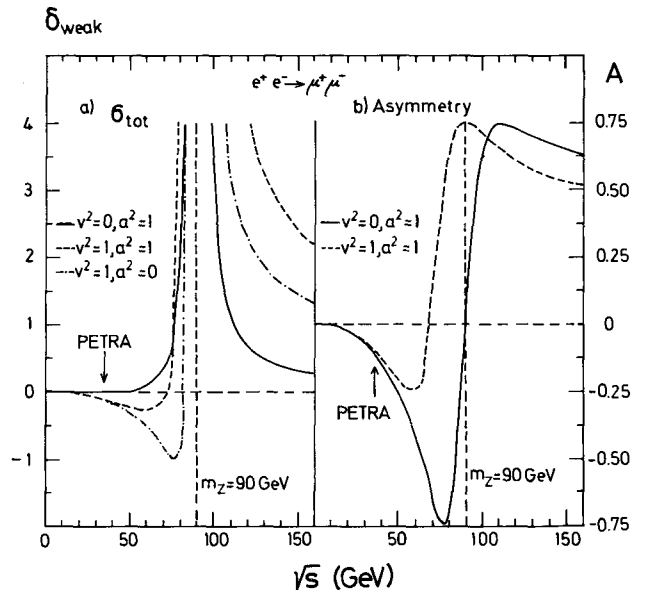
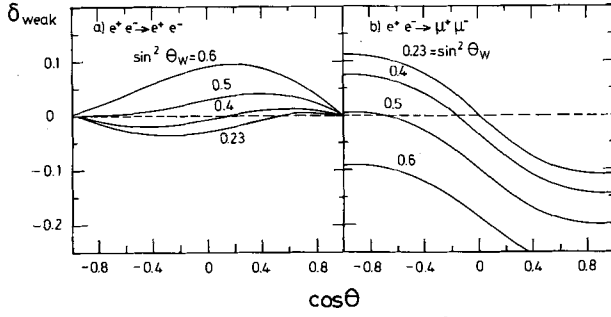


Fig. 13 a and b. The correction term  $\delta_{\text{weak}}$  in muon pair production for various values of  $v^2=4g_V^2$  and  $a^2=4g_A^2$  as a function of the centre-of-mass energy, a total cross section, b angular asymmetry

Figure 12 shows  $\delta_{\text{weak}}$ , (30), for Bhabha scattering at  $\sqrt{s}=35$  GeV for various values of  $v^2=4g_V^2$  and  $a^2=4g_A^2$ .  $\delta_{\text{weak}}$  vanishes at  $\theta=0^\circ$  and is negligibly small at  $\theta=180^\circ$ . It is also evident from Fig. 12 that a determination of  $v^2$  and  $a^2$  from Bhabha scattering will lead to a strong correlation between these two parameters, and that Bhabha scattering is somewhat more sensitive to  $v^2$  than to  $a^2$ . The  $s$ -dependence of  $\delta_{\text{weak}}$  can be taken from Fig. 13 which we have extended to very high energies to show the dramatic behaviour near the  $Z^0$  mass ( $m_z=90$  GeV). Figure 13a shows  $\delta_{\text{weak}}$ , (31), Fig. 13b the angular asymmetry  $A$ , (29), with  $x_1=1$ , for muon pair production. The arrows indicate the highest PETRA energy, where the electroweak



**Fig. 14 a and b.** The correction term  $\delta_{\text{weak}}$  at  $\sqrt{s} = 35$  GeV for some values of  $\sin^2\theta_w$  in the angular distribution for **a** Bhabha scattering, **b** muon pair production

effects become sizeable. The total lepton pair production cross section again is more sensitive to  $v^2$  whereas the angular asymmetry is sensitive to  $a^2$  since  $A = 0$  for  $a^2 = 0$ .

So far these formulae are model independent, except for the neglect of the  $Z^0$  width and the assumption of only one neutral weak boson. In order to get some estimates for the magnitude of expected weak effects, we specialize to the standard  $SU(2) \otimes U(1)$  electroweak theory, as proposed by Glashow, Salam and Weinberg [29], which has been extremely successful in the description of low  $|q^2|$  data [32].

In standard  $SU(2) \otimes U(1)$ ,  $G_V$  and  $G_A$  are expressed via a single parameter,  $\theta_w$ , the weak mixing angle, as

$$G_V = \frac{\sqrt{\pi\alpha}(1 - 4\sin^2\theta_w)}{\sin(2\theta_w)}, \quad G_A = \frac{-\sqrt{\pi\alpha}}{\sin(2\theta_w)} \quad (33a)$$

and therefore with the identification (24a)

$$m_z^2 = \frac{2\sqrt{2}\pi\alpha}{G_F \sin^2(2\theta_w)}, \quad (33b)$$

$$\Gamma_z = G_F m_z^3 \frac{\sqrt{2}}{3\pi} N \left( 1 - 2\sin^2\theta_w + \frac{8}{3}\sin^4\theta_w \right),$$

where  $N$  denotes the number of quark- and lepton generations,

$$v = 2g_V = 1 - 4\sin^2\theta_w, \\ a = 2g_A = -1.$$

Experimental  $\nu$ -scattering data [32] determine  $\sin^2\theta_w = 0.23$ . Inserting this value we get

$$m_z = 88.6 \text{ GeV}, \quad \Gamma_z = 2.5 \text{ GeV}, \\ v^2 = 4g_V^2 = 0.0064, \quad a^2 = 4g_A^2 = 1.$$

Since  $\sin^2\theta$  is close to  $1/4$ ,  $v^2$  is almost 0. Therefore the effects from standard electroweak theory on QED are represented in Figs. 12 and 13 by the curves  $v^2 = 0$ ,  $a^2 = 1$ .

Figure 14 shows once more  $\delta_{\text{weak}}$ , now with  $\sin^2\theta_w$  as a parameter. The variation of the differential cross

section due to  $\sin^2\theta_w$  is largest in lepton pair production. Assuming a value of  $\sin^2\theta_w = 0.23$ , then at current PETRA energies of  $\sim 35$  GeV the influence of the weak interaction is still quite small;  $\delta_{\text{weak}} = -3\%$  at  $\theta = 90^\circ$  for Bhabha scattering and  $\delta_{\text{weak}} = \pm 11\%$  at  $\theta = 0^\circ, 180^\circ$  for lepton pair production. In the total cross section for lepton pair production  $\delta_{\text{weak}}$  is negligibly small. It also follows that a measurement of  $\sin^2\theta_w = 0.23$  to better than 10% will be virtually impossible at PETRA. It is noted that that  $\delta_{\text{weak}}$  is not much larger than the uncertainty in the calculation of  $\delta_{\text{had}}$  (see p. 285).

## 5.2. Experimental Results

The results of the five PETRA experiments CELLO [9], JADE [5], MARK J [6], PLUTO [7] and TASSO [8] concerning weak interaction parameters are discussed in the following [30, 31, 38]. The sensitivity of the experiments to these parameters can be estimated by comparing Figs. 12–14 to the data shown in Figs. 6, 8, and 9. Obviously the present statistics are not good enough to determine even a single parameter of the weak interaction precisely. It is important, however, that the present experiments can give bounds on weak interaction parameters, thereby testing any model of the weak interaction at large values of  $|q^2|$ , which are not accessible in low energy experiments with stationary targets. We order the different analyses according to increasing complexity and include only results obtained from simultaneously fitting Bhabha scattering and lepton pair production. The determination of bounds on the weak mixing angle  $\theta_w$  obtained by the CELLO-group [24] is based on Bhabha scattering only (see Table 6).

The cross section studies include small luminosity corrections because the luminosity is monitored via small angle Bhabha scattering, hence slightly dependent on the electroweak model. It is assumed in these studies that QED is valid to any order of  $\alpha$  ( $A_+ = A_- = \infty$ ) and that the hadronic vacuum polarization is described correctly by (9) and (11). Furthermore, radiative corrections of weak terms are assumed to be small and ignored. The width of the  $Z^0$  boson is neglected.

Before discussing the analyses of the combined lepton pair data we note that the  $\mu$  pair asymmetry  $A$  (29) alone gives already valuable information on the axial vector coupling constant  $|g_A|$  and/or the  $Z^0$ -mass  $m_z$ . By neglecting terms in  $R^2$  and  $v \cdot R$  we can write to good approximation even at the highest PETRA energies:

$$A \approx \frac{3}{2} a^2 R = 6g_A^2 g m_z^2 \frac{s}{s - m_z^2} \xrightarrow{m_z \rightarrow \infty} -6g_A^2 g s. \quad (29')$$

With additional assumptions the following conclusions can be drawn from the measured asymmetry  $A$  (see Table 3):

- i*) If  $g_A^2 = \frac{1}{4}$  [i.e. equal to the prediction of the standard model, (33b)], then the lower limit on  $m_z$  is already 59 GeV (95% C.L.).
- ii*) If  $m_z$  is set to infinity – which is the most unfavourable case, then  $|g_A| < 0.56$  (95% C.L.)
- iii*) If the assumption of  $\mu$ - $e$ -universality is abandoned, the coupling-constant  $|g_A|^2$  has to be replaced by  $g_A^e \cdot g_A^\mu$ . By setting  $|g_A^e| = \frac{1}{2}$  and  $m_z = \infty$  one gets:  $|g_A^\mu| < 0.63$  (95% C.L.).

The above limits are preliminary and have been reported by the MARK J collaboration [30, 31].

As a side-remark it is pointed out that averaging the asymmetry measurements of all 4 experiments (see Table 3) is dangerous, since  $A$  depends on the respective acceptance intervals. Moreover, the systematic errors of the different experiments are possibly correlated.

We now proceed in describing the analyses of the complete set of lepton data of each experiment. In a first step the data were fitted to standard  $SU(2) \otimes U(1)$  with  $\sin^2 \theta_w$  as a free parameter, using (25), (26) with (28) and (33). Table 6 summarizes the experimental bounds on  $\sin^2 \theta_w$ . All groups find non-trivial bounds on  $\sin^2 \theta_w$  and no indication for a break-down of the model at  $|q^2| \sim 1200 \text{ GeV}^2$ .

In a second step the data were fitted in a more general way with the squared coupling constants  $g_V^2$  and  $g_A^2$ , using (25) and (26) with (28). The data are not sensitive to the third parameter  $m_z$ , except that it must be greater than 50 GeV. Therefore it was assumed that  $m_z^2 \gg s, q^2, \Gamma_z = 0$ . The results are given in Table 7. We have discussed earlier that the values obtained for  $g_V$  and  $g_A$  may be correlated. This is indeed the case as can be seen in Fig. 15, which will be discussed in more detail in the following.

The data still do not allow more than only qualitative statements about the weak coupling constants and more data is desirable, especially in lepton pair production. The MARK J collaboration, however, proposed a test which allows a more interesting conclusion. The neutral current amplitude in  $e^+e^-$  annihilation, (24), is closely linked with  $\nu\ell$  scattering via [34]

$$M_{nc}^{\nu\ell} = \frac{G_F m_z^2}{\sqrt{2}} \frac{1}{q^2 - m_z^2} \{ \bar{\nu} \gamma_\mu (1 + \gamma_5) \nu \bar{\ell} \gamma^\mu (g_V + g_A \gamma_5) \ell \} \quad (34)$$

in the case of only one  $Z^0$  boson. It turns out that the differential cross section in  $\nu\ell$  scattering is symmetric with respect to  $g_V$  and  $g_A$ . Hence two solutions are obtained in which  $g_V$  and  $g_A$  are exchanged:  $g_V \sim 0, g_A \sim -1/2$ , or  $g_V \sim -1/2, g_A \sim 0$ . This ambiguity is re-

**Table 6.** Experimental limits on  $\sin^2 \theta_w$  for  $s$  up to 36.7 GeV obtained from simultaneous fits to Bhabha scattering and lepton pair production. The results of the CELLO group are based on Bhabha scattering only

Group	Limits on $\sin^2 \theta_w$ (68% C.L.)		Ref.
	lower	upper	
CELLO	$> 0.12$	$< 0.38$	[24]
JADE	$> 0.10$	$< 0.40$	[20]
MARK J	$> 0.12$	$< 0.36$	[21]
PLUTO		$< 0.44$	[22]
TASSO	$> 0.13$	$< 0.35$	[23]

**Table 7.** Experimental limits on  $g_V^2$  and  $g_A^2$  for  $\sqrt{s}$  up to 36.7 GeV obtained from simultaneous fits to Bhabha scattering and lepton pair production

Group	$g_V^2 = v^2/4$	$g_A^2 = a^2/4$	Ref.
JADE	$0.01 \pm 0.08$	$0.18 \pm 0.16$	[20]
MARK J	$-0.04 \pm 0.09$	$0.20 \pm 0.16$	[21]
PLUTO	$-0.02 \pm 0.17$	$-0.19 \pm 0.24$	[22]
TASSO	$-0.14 \pm 0.12$	$0.25 \pm 0.14$	[23]

solved in favour of solution 1 [which coincides with the prediction of standard  $SU(2) \otimes U(1)$ ], if lepton-hadron processes are included in the analysis [32, 2].

In Fig. 15 the 95% confidence ellipses for  $g_V^2$  and  $g_A^2$  are displayed as obtained by the JADE, MARK J and PLUTO collaborations [20–22]. The central values for  $g_V^2$  and  $g_A^2$  of all 4 experiments (including TASSO [23]) are indicated in the figure with different symbols. The uncorrelated error bars for the TASSO-experiment are not shown, but they are comparable with the JADE and MARK J results (see Table 7). The hatched areas in Fig. 15 correspond to 95% contour curves for solution 1 and 2 of  $\nu\ell$ -scattering experiments.

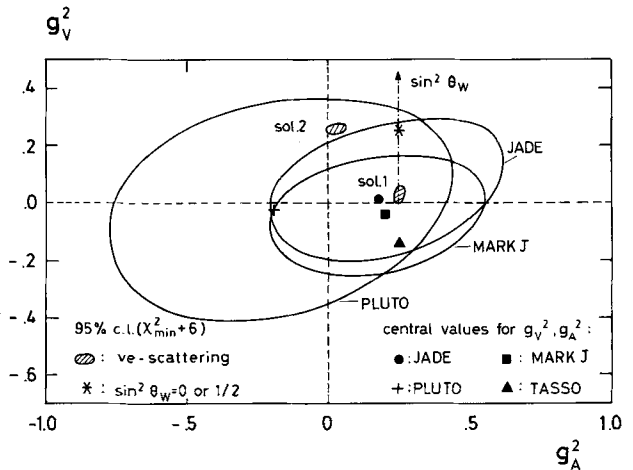


**Fig. 15.** 95% confidence contours of  $g_V^2$  and  $g_A^2$  for  $\sqrt{s}$  up to 36.7 GeV (see text for more explanations)

The Glashow-Salam-Weinberg prediction for  $g_V^2$ ,  $g_A^2$  [see (33b)] is also given in the figure (dashed-dotted line). Since  $g_V^2$  is a double valued function of  $\sin^2\theta_w$  in the model, any point on this line corresponds to two values of the Weinberg angle  $\theta_w$ , e.g.: if  $\sin^2\theta_w=0$  or 0.5, then  $g_V^2=0.25$  (asterisk in the figure). The accepted value  $\sin^2\theta_w=0.23$  from neutrino-hadron or  $eD$  scattering experiments yields:  $g_V^2=0.0016$ ,  $g_A^2=0.25$ , well within the hatched area of solution 1.

By inspection of Fig. 15 one concludes that the PETRA data are only compatible with solution 1.

The  $Z^0$ -field couples not only to leptons but also to hadrons. The vector and axial vector coupling constants can be expressed in terms of the Weinberg angle [33]. Hence the  $R$ -value which is defined as the ratio between the total hadronic and the  $\mu^+\mu^-$ -QED cross section gives also information on  $\sin^2\theta_w$ . Recent results of the JADE [20] and MARK J [21] collaborations indicate that the hadronic data at highest PETRA energies restrict the Weinberg angle to 68% C.L. intervals of

$$\text{JADE: } 0.11 \leq \sin^2\theta_w \leq 0.33$$

$$\text{MARK J: } 0.19 \leq \sin^2\theta_w \leq 0.61$$

It is important to note that these non-trivial limits on  $\sin\theta_w$  are obtained from the coupling of the neutral vector boson to all quarks and not only to  $u$ - and  $d$ -quarks as studied in neutrino scattering experiments.

### 5.3. Theories with Several Neutral Vector Bosons

The data have also been analyzed in the framework of more general gauge models in which several neutral vector bosons are allowed. For example, two groups of models extend the standard  $SU(2)\otimes U(1)$  group either to  $SU(2)\otimes U(1)\otimes SU(2)'$  [35], or  $SU(2)\otimes U(1)\otimes U(1)'$  [36]. Both of these models reduce to the standard model for  $|q^2|\rightarrow 0$  and the effective Lagrangian may be written as

$$L_{nc}^{eff} = \frac{4G_F}{\sqrt{2}} \{ (j^{(3)} - \sin^2\theta_w j_{em})^2 + C j_{em}^2 \},$$

where  $j^{(3)}$  is the 3rd component of the weak isospin current and  $j_{em}$  the electromagnetic current.  $C$  measures the deviation from the standard model and is related to the coupling constants and masses of the particular model.

If one specializes to the case of only two neutral vector bosons with masses  $m_1 < m_2 < m_Z$ ,  $C$  can be expressed as

$$C = \gamma \frac{(m_2^2 - m_Z^2)(m_Z^2 - m_1^2)}{m_1^2 m_2^2}, \quad (35)$$

**Table 8.** 95% C.L. limits on the parameter  $C$  in multi-gauge boson models

Group	Limits on $C$	Ref.
JADE	$<0.039$	[20]
MARK J	$<0.032$	[21]
PLUTO	$<0.06$	[22]
TASSO	$<0.03$	[23]

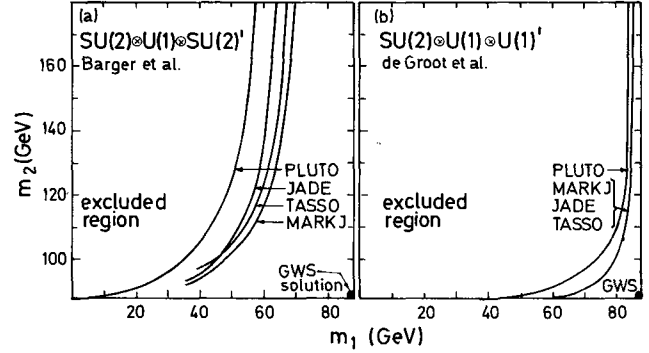


**Fig. 16 a and b.** The 95% confidence level contours for a fit to the two gauge boson models of **a** Barger et al. and **b** de Groot et al.

where  $\gamma$  can be chosen as

$$\gamma = \sin^4\theta_w \quad \text{or} \quad \gamma = \cos^4\theta_w$$

if one allows for two charged and two neutral gauge bosons or one charged and two neutral bosons, respectively [35, 36].

The differential cross sections for Bhabha scattering and  $\mu$  pair production may be parameterized in terms of  $C$  and  $\sin^2\theta_w$  [37]. A good approximation at current PETRA energies is to substitute in the single gauge boson formulae (25) and (26)  $v^2$  by  $v^2 + 16C$ , and to leave  $a^2$  unchanged. Fixing  $\sin^2\theta_w=0.23$  the parameter  $C$  can be fitted and by using (35) bounds for  $m_1$  and  $m_2$  are obtained. The results for  $C$  from the different PETRA groups are listed in Table 8.

The bounds in the corresponding  $m_1$  versus  $m_2$  plot are displayed in Fig. 16. The excluded mass regions for the particular models are indicated in the figure. We see that the PETRA data restrict the mass range of 2 neutral bosons quite appreciably. Since the lepton boson coupling in the  $SU(2)\otimes U(1)\otimes U(1)'$  model is  $\sim \cos^4\theta_w$ , and therefore much stronger than for the  $SU(2)\otimes U(1)\otimes SU(2)'$  model ( $\sim \sin^4\theta_w$ ), the data restrict both masses in the former case to values close to  $m_Z$ . The conclusions one can draw for the latter case are much weaker.

## 6. Conclusions

After the second year of experimentation at PETRA the following conclusions can be made: there is no sign

of unanticipated deviations from QED up to  $s, |q^2| \sim 1300 \text{ GeV}$ . There is good evidence that the  $\tau$  is a pointlike sequential lepton. The expected deviations from QED due to the weak neutral current are still smaller than the statistical errors. The limits obtained on the vector and axial vector coupling constants of the weak interaction are a first test of electroweak theories at large  $s$  and  $|q^2|$ .

*Acknowledgements.* We are greatly indebted to our colleagues from CELLO, JADE, MARK J, PLUTO and TASSO who furnished the information from their respective experiments. We are very grateful to Dr. F. Gutbrod for many helpful discussions. We thank Dr. W. Bartel, Prof. A. Böhm, Prof. G. Flügge, P. Grosse-Wiesmann, Prof. H. Meyer, Dr. L. H. O'Neill, Dr. M. Pohl, Prof. P. Soding, Prof. H. Spitzer and Dr. G. Wolf for a critical reading of the manuscript. One of us, V.H., wishes to thank the DESY directorate for the hospitality extended to him during his stay in Hamburg.

## References

- J. Bailey et al.: Nucl. Phys. **B150**, 1 (1979)
- C.Y. Prescott et al.: Phys. Lett. **77B**, 347 (1978)
- J.E. Augustin et al.: Phys. Rev. Lett. **34**, 233 (1975)  
T. Himel et al.: Phys. Rev. Lett. **41**, 449 (1978)  
L.H. O'Neill et al.: Phys. Rev. Lett. **37**, 395 (1976)  
B.L. Beron et al.: Phys. Rev. **D17**, 2187, 2839 (1978)
- DASP-Collaboration R. Brandelik et al.: Z. Phys. C – Particles and Fields **1**, 233 (1979)
- JADE-Collaboration W. Bartel et al.: Phys. Lett. **88B**, 171 (1979)
- MARK J-Collaboration D.P. Barber et al.: Phys. Rev. **63**, 337 (1980)
- PLUTO-Collaboration Ch. Berger et al.: Z. Phys. C – Particles and Fields **4**, 269 (1980)
- TASSO-Collaboration R. Brandelik et al.: Phys. Lett. **83B**, 261 (1979)
- CELLO-Collaboration M.J. Schachter: DESY-Report 80–128 (1980)
- See e.g. the chapter on quantum electrodynamics in S.S. Schweber: An introduction to relativistic quantum field theory. New York: Harper and Row 1962
- F.A. Berends, K.F.J. Gaemers, R. Gastmans: Nucl. Phys. **B63**, 381 (1973)  
F.A. Berends, K.F.J. Gaemers, R. Gastmans: Nucl. Phys. **B68**, 541 (1974)  
F.A. Berends, R. Kleiss: DESY-Report 80–66 (1980)
- K. Sauerberg: Ph. D. Thesis, DESY Internal Report F22-79/01 (1979)
- F.A. Berends, G.J. Komen: Phys. Lett. **63B**, 432 (1976)
- W. Bartel et al.: Phys. Lett. **88B**, 171 (1979),  
D. Cords: DESY Report 80/92 (1980)  
D.P. Barger et al.: Phys. Rev. Lett. **43**, 901 (1979)  
Ch. Berger et al.: Phys. Lett. **81B**, 410 (1979)  
R. Brandelik et al.: Phys. Lett. **88B**, 199 (1979); Z. Phys. C – Particles and Fields **4**, 87 (1980)  
H.-J. Behrend et al.: To be published
- S.D. Drell: Ann. Phys. **4**, 75 (1958)
- N.M. Kroll: Nuovo Cimento **45A**, 65 (1966)  
R. Hofstadter: Proc. Stanford Conf. 869 (1975)  
K. Ringhofer, H. Salecker: Contr. paper 109 to the Stanford Conf. 1975;  
R.F. Schwitters. Proc. Tbilisi Conf. B34 (1976)
- A. Litke: Harvard University, Ph. D. Thesis (1970) (unpublished)
- J. Takahashi: Nuovo Cimento **6**, 370 (1957)
- F.E. Low: Phys. Rev. **110**, 974 (1958)
- JADE-Collaboration W. Bartel et al.: Phys. Lett. **92B**, 206 (1980); Phys. Lett. **99B**, 281 (1981); DESY-Report 81-015 (1981) (to be published).  
R. Marshall: Private communication
- MARK J-Collaboration D.P. Barber et al.: Phys. Rev. Lett. **43**, 1915 (1979); Phys. Lett. **95B**, 149 (1980); PITHA 81/07 (1981) (to be published); private communication M. Pohl and F.P. Poschmann
- PLUTO-Collaboration Ch. Berger et al.: Z. Phys. C – Particles and Fields **1**, 343 (1979); Z. Phys. C – Particles and Fields **7**, 289 (1981); Phys. Lett. **94B**, 87 (1980); Phys. Lett. **99B**, 489 (1981)
- TASSO-Collaboration R. Brandelik et al.: Phys. Lett. **92B**, 199 (1980); Phys. Lett. **94B**, 259 (1980); private communication C. Youngman, H. U. Martyn, M. Ogg
- CELLO-Collaboration H.-J. Behrend et al.: DESY Report 81-021 (1981) (submitted to Phys. Lett. B)
- K. Koller, T.F. Walsh, P.M. Zerwas. DESY Internal Report T-79/1 (1979) (unpublished)
- DELCO-Collaboration W. Bacino et al.: Phys. Rev. Lett. **42**, 749 (1979)
- C. Jarlskog, F.J. Yndurain: Phys. Lett. **63B**, 215 (1976)
- R. Budny: Phys. Lett. **55B**, 227 (1975)
- S.L. Glashow: Nucl. Phys. **22**, 579 (1961); Rev. Mod. Phys. **52**, 539 (1980)  
A. Salam. Phys. Rev. **127**, 331 (1962); Rev. Mod. Phys. **52**, 525 (1980)  
S. Weinberg: Phys. Rev. Lett. **19**, 1264 (1967); Rev. Mod. Phys. **52**, 515 (1980)
- A. Böhm: Proc. of the Intern. Conf. on High Energy Physics, p. 551, Madison, 1980: PITHA-Report 80/9 (1980)
- M. Pohl: XVI Rencontre de Moriond, Les Arcs, 1981, PITHA-Report 81/10 (1981) (to be published)
- General references on analyses of neutrino scattering data:  
K. Winter: Proc. of the 1979 Intern. Symposium on Lepton and Photon Interactions, Fermilab p. 258 (1979)  
In addition: H. Faissner: New phenomena in lepton-hadron physics, p. 371; ed. D.E. Fries, J. Wess, New York: Plenum 1979  
H. Reither. Phys. Bl. **35**, 630 (1979)  
F.W. Bullock: Proc. of Neutrino 79, p. 398, Bergen 1979  
R.H. Heisterberg et al.: Phys. Rev. Lett. **44**, 635 (1980)  
L.W. Mo: Contribution to Neutrino 80, Erice (1980)  
P. Langacker et al.: Proc. of Neutrino 79, p. 276, Bergen, 1979  
M. Roos, I. Liede. Phys. Lett. **82B**, 89 (1979) and references therein
- J. Ellis, M.K. Gaillard: Physics with very high energy  $e^+e^-$  colliding beams. CERN 76-18 (1976) 21
- L. Wolfenstein: Proc. AIP-Conference on Particles and Fields, Williamsburg, 1974
- V. Barger, W. Y. Keung, E. Ma: Phys. Rev. Lett. **44**, 1169 (1980)
- E.H. de Groot, D. Schildknecht, G.J. Gounaris: Phys. Lett. **90B**, 427 (1980)
- E.H. de Groot, D. Schildknecht: Phys. Lett. **95B**, 128 (1980)
- Earlier PETRA results on QED and electroweak effects have been reviewed by:  
R. Marshall: XV Rencontre de Moriond, Les Arcs, 1980 and Rutherford Lab. preprint RL-80-029  
P. Dittmann: Warsaw Symp. on Element. Part. Phys., Jodlowy Dwór, May 1980  
V. Hepp: Mainz Symp. on Status of QED, May 1980 and published in Lecture Notes in Physics, 143, p. 35, ed. G. Gräff, E. Klempt, G. Werth. Berlin, Heidelberg, New York: Springer 1981